Comprehensive multidimensional liquid chromatography-mass spectrometry for the characterization of charge variants of a bispecific antibody

Grunert, I.; Heinrich, K.; Hingar, M.; Ernst, J.; Winter, M.; Bomans, K.; ... ; Bulau, P.

ACS Partner Journal

Journal of the American Society for Mass Spectrometry

pubs.acs.org/jasms

Research Article

Comprehensive Multidimensional Liquid Chromatography–Mass Spectrometry for the Characterization of Charge Variants of a Bispecific Antibody

Published as part of the Journal of the American Society for Mass Spectrometry virtual special issue "High-Throughput in Mass Spectrometry".

Ingrid Grunert,* Katrin Heinrich, Michael Hingar, Juliane Ernst, Martin Winter, Katrin Bomans, Katharina Wagner, Arnaud Fevre, Dietmar Reusch, Manfred Wuhrer, and Patrick Bulau

Cite This: *J. Am. Soc. Mass Spectrom.* 2022, 33, 2319–2327

Read Online

ACCESS | Metrics & More | Article Recommendations | Supporting Information

ABSTRACT: Identification and further characterization of antibody charge variants is a crucial step during biopharmaceutical drug development, particularly with regard to the increasing complexity of novel antibody formats. As a standard analytical approach, manual offline fractionation of charge variants by cation-exchange chromatography followed by comprehensive analytical testing is applied. These conventional workflows are time-consuming and labor-intensive and overall reach their limits in terms of chromatographic separation of enhanced structural heterogeneities raised from new antibody formats. For these reasons, we aimed to develop an alternative online characterization strategy for charge variant characterization of a therapeutic bispecific antibody by online mD-LC-MS at middle-up (2D-LC-MS) and bottom-up (4D-LC-MS) level. Using the implemented online mD-LC-MS approach, all medium- and even low-abundant product variants previously identified by offline fraction experiments and liquid chromatography mass spectrometry could be monitored. The herein reported automated online mD-LC-MS methodology therefore represents a complementary and in part alternative approach for analytical method validation including multiattribute monitoring (MAM) strategies by mass spectrometry, offering various benefits including increased throughput and reduced sample handling and combined protein information at intact protein and peptide level.

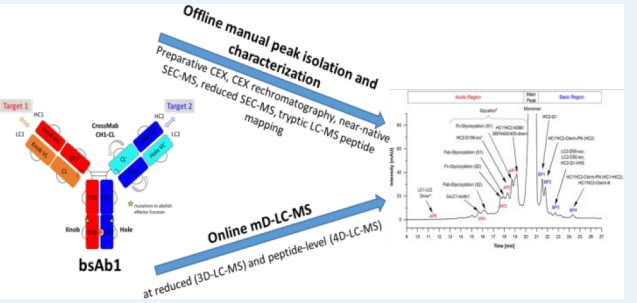

KEYWORDS: *cation-exchange chromatography, multidimensional liquid chromatography, mass spectrometry, online HPLC, automation, product variants, bispecific antibodies, critical quality attributes, multiattribute monitoring*

For decades, monoclonal antibodies (mAbs) have been produced and marketed for application in numerous clinical treatments. Their success led to the development and engineering of several new, more complex formats such as bispecific antibodies (bsAbs), polyclonal antibodies, antibody fragments (Fabs, nanobodies), and antibody–drug conjugates (ADCs).[1]

BsAbs simultaneously bind two different epitopes or targets.[1] Therefore, various techniques exist to accomplish their heterodimerization of heavy chains (HCs) and the assembly of light chains (LCs) to the corresponding HCs (e.g., knob-into-hole or CrossMab design).[2−4] This leads to enhanced structural heterogeneity during manufacturing, expressed by various process- and product-related byproducts, accordingly often reflected in complex analytical methods to ensure adequate removal or reduction to acceptable levels. Besides structural variants, such as fragments or aggregates, acidic and basic charge variants may occur.[5]

As a standard analytical procedure, isolation and related enrichment of these heterogeneous species by offline peak fractionation, e.g., by ion-exchange chromatography (IEX) for charge variants or size-exclusion chromatography (SEC) for size variants and subsequent mass spectrometric (MS) characterization, is applied.[6] Cation-exchange chromatography (CEX) is the most commonly used analytical tool for the characterization and quantification of protein charge variants.[7] Charge variants are predominantly caused by glycosylation, lysine glycation, asparagine deamidation, aspartate isomerization, and further post-translational modifications (PTMs).[6,7]

Received: October 14, 2022
Revised: October 18, 2022
Accepted: October 20, 2022
Published: November 28, 2022

In addition, these may include degradations and higher order structure alterations, such as fragments and aggregates.[8] The variety of species poses a substantial challenge for state-of-the-art chromatography and identification of specific product variants. Moreover, insufficient chromatographic separation of multiple charge variants complicates their identification and subsequent functional characterization. This leads to the demand of deploying a combination of different analytical techniques and methods, including technical improvements during development.

To overcome these challenges, online multidimensional liquid chromatography coupled to MS (mD-LC-MS) has been utilized as an alternative approach enabling fast automated online characterization by combining different separation mechanisms.[9,10] Several studies outline the mD-LC-MS analysis of host cell proteins, isolation of mAbs from complex matrices, and mAb or ADC characterization, proceeding at the top-down, middle-up, or bottom-up level employing different chromatographic steps (e.g., SEC, IEX, hydrophilic or hydrophobic interaction) in their first dimension (^{1}D).[9,10] Various publications show numerous advantages, including improved resolution capacity and time savings compared to standard offline one-dimensional LC,[11,12] whereas consistently new application fields of mD-LC-MS emerge.[9,12] Recent work has demonstrated the feasibility of mD approaches for the characterization of conventional mAbs. Gstöttner et al.[13] described the characterization of five standard mAb charge variants using mD-LC-MS. Goyon et al.[14] reported further improvements of the mD approach by characterization of seven antibodies (including IgG1, IgG2, and IgG4).

Hence, the present study focuses on the development of an improved mD-LC-MS approach for the systematic characterization of heterogeneous bsAb charge variant profiles. We optimized and automated peak fractionation to make the best use of the chromatographic separation. The mD-LC-MS approach allowed a comprehensive characterization of bsAb charge variants, similar to the more laborious and time-intensive offline approach.

EXPERIMENTAL SECTION

bsAb1. The recombinant bispecific IgG1 antibody (bsAb1) was expressed in a chinese hamster ovary cell system and manufactured at Roche Diagnostics, Penzberg, Germany, using standard cell culture and purification technology. The drug substance material was formulated at a concentration of 123 mg/mL in a His/acetate buffer system (20 mM) at pH5.5, whereas drug product material was formulated at a concentration of 120 mg/mL.

mD-LC-MS System (2D- and 4D-LC-MS). *Instrumentation.* An extended Agilent Technologies Infinity LC System was used for mD-LC-MS analysis controlled by OpenLAB CDS ChemStation (SR4) software from Agilent Technologies. Both Q Exactive HF (4D-LC-MS) and an Exactive EMR MS (2D-LC-MS) were controlled by Xcalibur software (Thermo Fisher).

The 2D-LC-MS system contains a 1260 Infinity II Bioinert Pump (^{1}D), a 1260 Quaternary Pump, and a 1260 Infinity II Highspeed Pump (^{2}D), whereas the 4D-LC-MS system contains a 1290 Infinity II Bioinert Pump (^{1}D), a 1260 Flexible Pump (^{2}D), a 1260 Cap Pump (^{3}D), and a 1260 Infinity II High Speed Pump (^{4}D). All capillaries with contact to samples are composed of PEEK or bioinert material, except for the stainless steel loops at the Multiple-Heart-Cutting Valve (MHC-Valve).

Workflow of Online mD-LC-MS Methods. *(^{1}D) Online CEX Separation and Fractionation.* BsAb1 charge variants were analyzed on a BioPro IEX-SF column (4.6 × 100 mm, 5 μm, YMC) with a flow rate of 0.8 mL/min and column temperature of 41 °C. 150 μg of bsAb1 was injected for the 2D-LC-MS setup and 4D-LC-MS main peak cuts, whereas 1000 μg was applied for 4D-LC-MS acidic and basic peaks. Separation was achieved with a gradient from 2% to 15% eluent B in 30 min, 15% to 100% in 0.1 and 5 min at 100% eluent B (eluent A: 20 mM *N*,*N*-bis(2-hydroxyethyl)taurine (BES), pH 6.8; eluent B: 20 mM BES, 488 mM NaCl, pH 6.8). Based on the ^{1}D UV280 nm chromatogram, the cuts were defined and collected in 40 μL (2D-LC-MS) or 120 μL (4D-LC-MS) loops of the MHC-Valve.

(^{2}D) Online RPLC Reduction for 2D- and 4D-LC-MS. Employing a valve plugin programed by ANGI (Gesellschaft für Angewandte Informatik mgH), all subsequent methods in a second ChemStation panel automatically started by switching the MHC-Valve to transfer the collected cuts onto the ^{2}D column (ZORBAX Stable Bond 300 C3, 4.6 × 12.5 mm, 5 μm, Agilent Technologies) within the 4D-LC-MS setup. For the 2D-LC-MS setup, an Acquity BEH C4 (2.1 × 50 mm, 1.7 μm) from Waters was implemented and the reducing agent (20 mM dithiothreitol, DTT) was added by the ^{2}D pump to reduce bsAb1 into heavy (HC1, HC2) and light chain (LC1, LC2) subunits at 80 °C. The separation of the bsAb1 chains is accomplished by an incorporated additional pump described in the following paragraph. In regard to the 4D-LC-MS setup, eluents A and B contained 0.1% formic acid (FA) in water (H_2O, eluent A) and acetonitrile (ACN, eluent B). Mobile phase C containing 20 mM DTT was used to reduce bsAb1 samples into HC and LC subunits. After a short flushing step, the reduced bsAb1 subunits were eluted by multiple gradients up to 45% eluent B within 50 min. With elution of the subunits the valve located between ^{2}D and ^{3}D column switched and the subunits were transferred with low flow to the ^{3}D trypsin cartridge (Poroszyme, 2.1 × 30 mm, Thermo Scientific).

(^{2}D) Separation of Reduced bsAb1 for 2D-LC-MS. BsAb1 reduced subunits were separated at 80 °C on an Acquity BEH C4 column (2.1 × 50 mm, 1.7 μm) from Waters with the following gradient: After a short flushing step with 1% B (0.1% FA in ACN, buffer A: 0.1% FA in H_2O), the bsAb1 chains were eluted with a multiple linear gradient from 1−28% B in 6 min, 28−32% B in 4 min, and 32−100% B in 7 min at a flow rate of 0.3 mL/min. With the elution of the subunits the diverter valve switched and the chains of bsAb1 were transferred to an EMR MS system.

(^{3}D) Tryptic Digestion for 4D-LC-MS. A Poroszyme immobilized trypsin cartridge (2.1 × 30 mm) supplied by ThermoFisher Scientific was employed and operated at 37 °C. Digestion buffer A consisted of 50 mM tris(hydroxymethyl)-aminomethan (TRIS) and 10 mM $CaCl_2$, pH8.0. Buffer B contained 0.1% FA in ACN. While receiving bsAb1 subunits from C3, the cartridge was also in line with ^{4}D peptide-mapping column. Hence, the resulting peptides from the trypsin cartridge (12 s residence time, flow-through mode) were trapped onto the ^{4}D column.

(^{4}D) RPLC Tryptic Peptide Mapping for 4D-LC-MS. The RPLC Poroshell 120 Bonus-RP (2.1 × 100 mm, 2.7 μm) applied for the tryptic peptide mapping analysis of the acidic cuts and the RPLC Poroshell 120 SB-C18 (2.1 × 100 mm, 2.7

https://doi.org/10.1021/jasms.2c00296
J. Am. Soc. Mass Spectrom. 2022, 33, 2319−2327

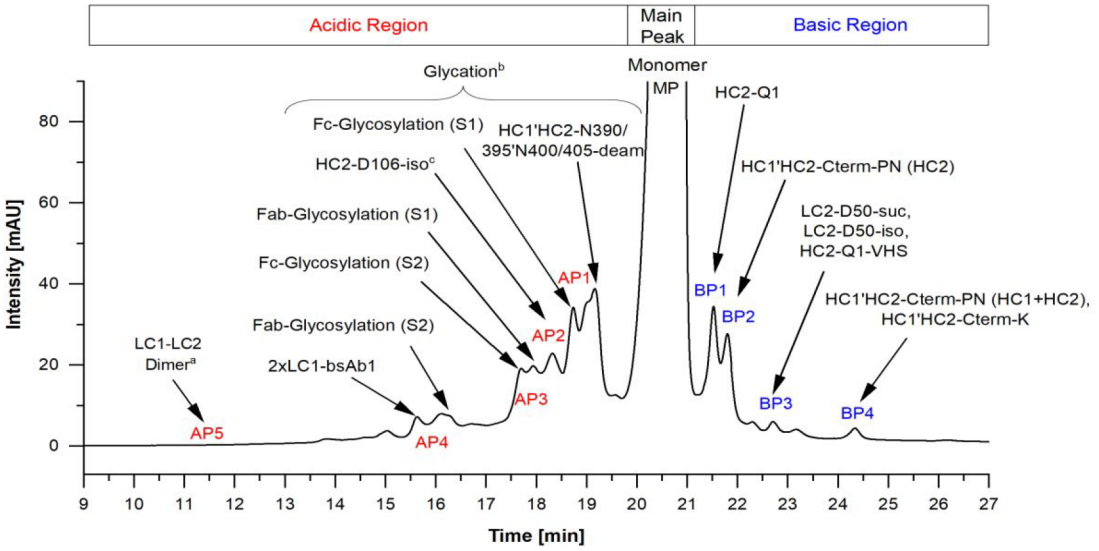

Figure 1. CEX-UV chromatogram of bsAb1 charge variant analysis summarizing the identified species and peak assignments using the standard release testing method. AP = acidic peak, BP = basic peak, S1 = monosialylated glycans, S2 = disialylated glycans. (a) identified by 2D-LC-MS and by spiking of fractionated LMW into CEX, (b) 162 Da shift due to glycation, (c) HC2-D106-iso identified by 4D-LC-MS of a drug product stability sample.

μm) used for the basic cuts were both supplied by Agilent Technologies. Mobile phases contained 0.1% FA in water (A) and ACN (B), respectively. The flow rate was set to 0.3 mL/min and the column temperature to 60 °C. At the beginning, the ^{4}D column was equilibrated with 1% B. After transfer and trapping of the peptides the valve switched back and the ^{4}D column was flushed with 1% B for 3 min. Subsequently, the trapped peptides were eluted with the following conditions: 1−40% B in 40 min, 40−65% B in 5 min, and transferred to a Q-Exactive HF MS system.

MS System Parameters and Data Analysis. Parameters for MS system detection were set according to experience available from reduced and peptide analysis of recombinant antibodies as outlined in Supporting Information Experimental Section S1. Data analysis was performed with the help of Protein Metrics software.

RESULTS AND DISCUSSION

Offline Characterization of bsAb1 Charge Variants. At first, offline CEX fractionation of bsAb1 reference material followed by an in-depth analytical characterization was performed to initially characterize and identify bsAb1 variants. BsAb1 exhibits a variety of acidic and basic charge species as depicted in the CEX-UV chromatographic profile (Figure 1). Five different acidic charge variant regions (AP1−5), the main peak variant (MP), and four basic peak areas (BP1−4) were assessed. To enable their identification, the CEX fractions were manually isolated by semipreparative CEX and further analyzed. In total, 200 fractionation runs were conducted to gain sufficient material of low abundant peaks, e.g., for basic peak 3 (BP3). Analytical CEX rechromatography enabled the verification of the corresponding CEX peaks including peak purity (Supporting Information Figure S1), near-native SEC-UV-MS and reduced reversed-phase chromatography coupled to mass spectrometry (RP-MS) identified bsAb1 size and glycan variants (Supporting Information Table S1), and tryptic LC-MS/MS peptide mapping (Supporting Information Table S2) elucidated post-translational amino acid modifications (PTMs). A combination of all these techniques was necessary to identify bsAb1's major charge variants and assign them to the respective CEX peak as summarized in Figure 1.

SEC-UV-MS at near-native and RP-MS at reduced levels of acidic fractions detected predominantly different glycosylation sites at the Fab and Fc part of the molecule. In comparison to the Fc-glycosylated main peak (G0F/G0F) at the intact level, the acidic fractions, AP3 and AP4, contained additional mass shifts attributed to secondary biantennary N-glycans incorporating one or two sialic acids (AP3: G1S1F, G2S1F and AP4: G2S2F), exemplarily shown in Supporting Information Figure S2. A supplementary RP-MS analysis of selected fractions after deglycosylation and reduction localized the Fab glycosylation to LC2 and discriminated that the observed 162 Da mass shift of acidic fractions (AP1, AP2, AP3) predominantly contained glycation (instead of Fc galactosylation, Supporting Information Table S3). Similarly, different sialylations of Fc glycans, namely mono- (G1S1F, G2S1F) and disialylated (G1S2F, G2S2F) glycans, were observed to elute at different retention times, AP1 (monosialylated species) and AP3 (disialylated species), respectively. This is in agreement with previous publications where it has been shown that sialylation and glycation introduce net negative charge resulting in an earlier elution.[7,15] Interestingly, the Fab glycosylation was predominantly perceived in intact SEC-MS, whereas the differences in Fc glycosylation seem to ionize better in reduced RP-MS. Moreover, it needs to be mentioned that acidic conditions and higher temperature as applied for reduced RP-MS might lead to hydrolysis of sialic acids and thus might affect the results compared to near-native SEC-MS. The intact analysis evaluates combined sugar moieties (glycoform pairs) compared to the individual glycans on each chain during reduced analysis. Fab glycosylation is a known recombinant antibody modification[16] and has been observed to elute in acidic region during IEX characterization of another therapeutic bispecific antibody as well.[15] Additionally, the intact bsAb1 data revealed a mispairing variant in AP4 that incorporates twice the LC1 (2xLC1-bsAb1: HC1-LC1/HC2-LC1) within the intact molecule, instead of the desired LC1/LC2 combination.[17] This assignment is supported at reduced RP-MS level by a

https://doi.org/10.1021/jasms.2c00296
J. Am. Soc. Mass Spectrom. 2022, 33, 2319−2327

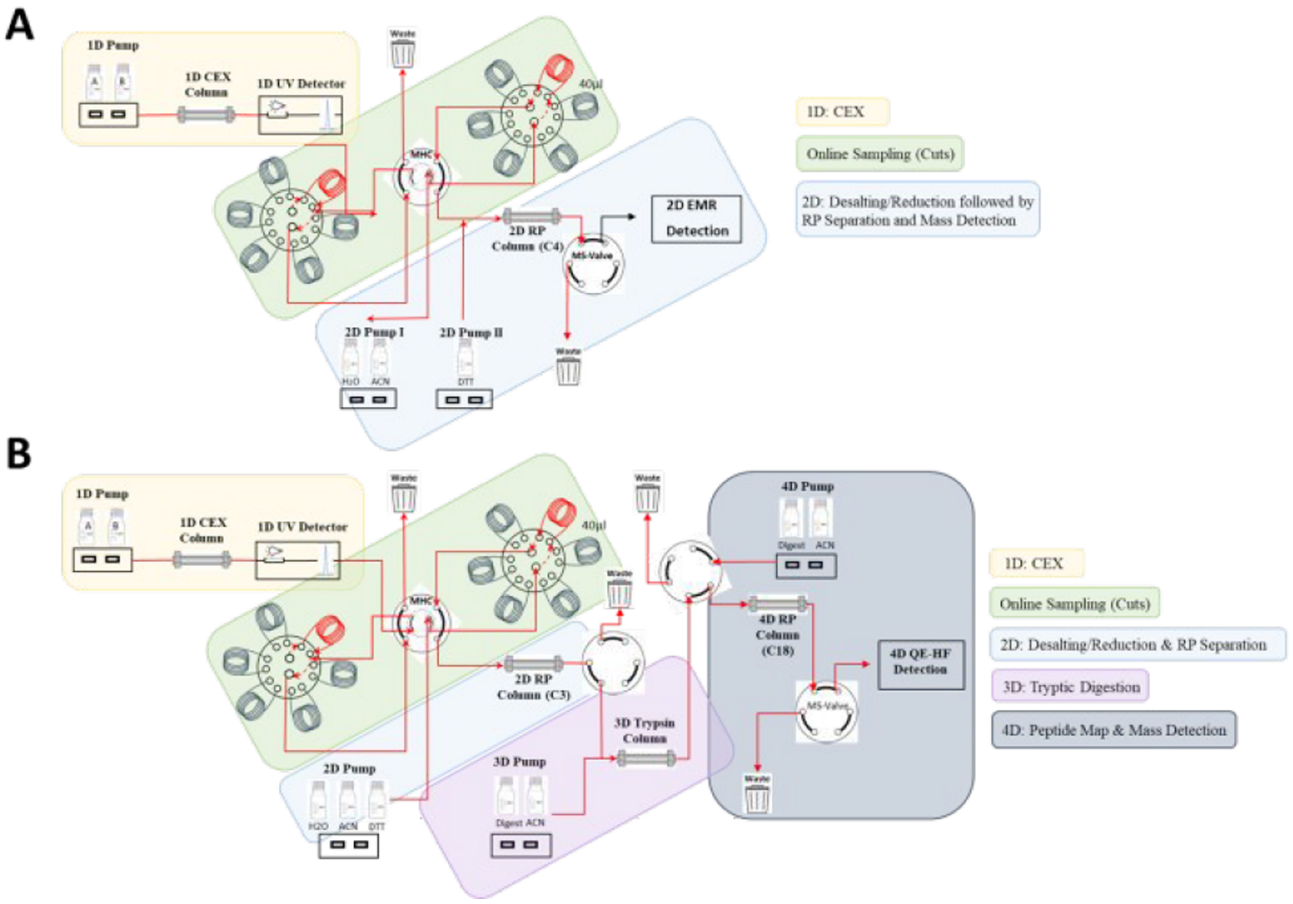

Figure 2. Schematic illustration of the online mD-LC-MS setup. (A) 2D-LC-MS setup incorporating ^{1}D CEX separation and charge variant peak collection, ^{2}D RPLC-based desalting and reduction, followed by RPLC (C4) separation and MS detection. (B) 4D-LC-MS setup incorporating ^{1}D CEX separation and peak collection, ^{2}D RPLC (C3) based desalting and reduction, ^{3}D tryptic digestion, and ^{4}D RPLC-MS/MS based peptide mapping.

decrease in LC2 and an increase in LC1 abundance (Supporting Information Table S1). The low-abundant AP5 region (<0.2% of total peak area) could not be assessed by manual peak fractionation. Spiking of a low-molecular weight SEC fraction into CEX resulted in an increase of AP5, identified in a parallel near-native SEC-UV-MS and native LysC peptide mapping analysis, a fragment composed of covalently linked LC1 and LC2 (LC1-LC2 dimer; data not shown). Both the 2xLC1-bsAb1 and LC1-LC2 dimer are known structural variants of bsAbs.[5,17,18] The elution of antibody fragments in the acidic region of IEX separations has also been reported recently.[7] Basic species were predominantly identified to comprise N- and C-terminal modifications, which is in accordance with the available literature:[6,7] BP1 shows an enrichment in the reformation of pyroglutamate to glutamine at HC2, BP2 retains proline amide (predominantly at HC2), and BP3 contains the N-terminal valine-histidine-serine (VHS) signal peptide at HC2 as well as a succinimide intermediate at LC2, and BP4 reveals almost complete proline amidation at both HCs (Supporting Information Table S1). As already observed for the acidic fractions, differences in abundance of bsAb1 species for reduced RP-MS versus near-native SEC-MS were observed. This phenomenon might be describable by different ionization efficiencies, charge changes due to modifications, and less chromatographic resolution of the intact SEC-MS (relative to the reduced RP-MS), as well as the molecular size differences between the intact and reduced level.[19,20]

Subsequently, tryptic LC-MS/MS peptide mapping of the offline charge variant fractions was applied to quantify PTMs (Supporting Information Table S2), particularly those exhibiting low mass alterations to the nonmodified parent peptides, assign them to the corresponding CEX peak, and identify them down to the amino acid level. The data revealed an enrichment of asparagine deamidation of the conserved Fc motif (CH3 domain)[21] found in both HCs (HC1'HC2-N390/395'N400/405-deam) for AP1. Deamidation of asparagine to aspartic acid introduces negative net charge resulting in an earlier elution.[7] The isomerization at aspartate 106 (HC2-D106-iso) showed constantly moderate levels, without an enrichment of a particular CEX offline fraction, and thus, an assignment to a specific CEX peak was not feasible. As expected, the peptide mapping data confirmed the N- and C-terminal modifications observed by the preceding SEC-MS analysis: reformation of pyro-glutamate to glutamic acid at HC2 (~50% HC2-Q1) was assigned to BP1, within BP2 proline amidation at around 30% was identified and BP3 contained the proposed N-terminal VHS signal peptide at HC2 (~20% HC2-Q1-VHS) as well as the succinimide formation at LC2-D50 (~15% LC2-D50-suc). In addition to the observed succinimide, the respective complete isomerization to iso-aspartic acid (~10% LC2-D50-iso) was identified to increase as well. BP4 showed almost complete proline

https://doi.org/10.1021/jasms.2c00296
J. Am. Soc. Mass Spectrom. 2022, 33, 2319−2327

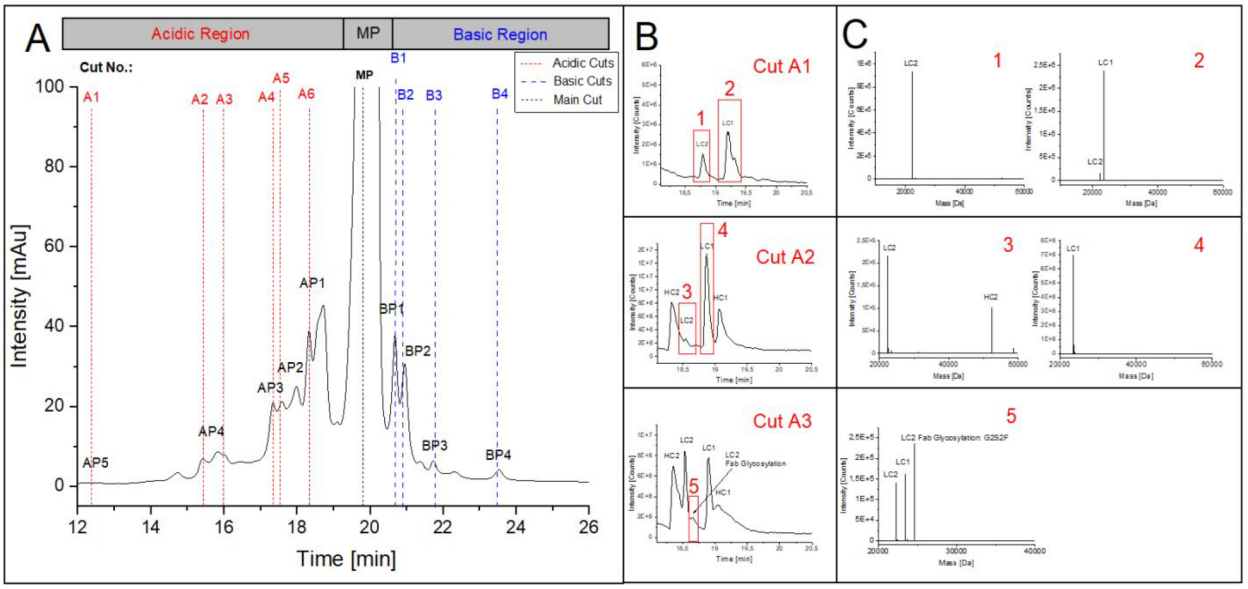

Figure 3. Online 2D-LC-MS analysis of bsAb1. (A) CEX-UV chromatogram of bsAb1 ([1]D) highlighting collected cuts (7 s sampling time, AP5:9 s): red: cuts of acidic charge variants (A1-A6); blue: cuts of basic charge variants (B1−B4); black: cut of main peak (MP), including analytical CEX peak naming (black). (B) [2]D total-ion-current (TIC) chromatograms of reduced bsAb1 exemplarily shown for selected [1]D cuts as depicted. (C) corresponding deconvoluted mass spectra of modified bsAb1 chain(s).

amidation (~70% HC1'HC2-Cterm-PN) and further identified a minor enrichment of C-terminal lysine (~5% HC1'HC2-Cterm-K) that was not observed by intact or reduced analysis before. Moderate levels of oxidation (sum of both oxidation sites: ~5−10%) were observed for all analyzed CEX fractions. MS/MS data assessment confirmed the described amino acid modifications. Similarly, as observed before, the abundance of charge variants at the peptide level slightly varies compared to the intact and reduced analysis. These quantitative differences are most likely a result of ionization efficacy alterations at the intact versus peptide level and have been reported before.[15,22]

In summary, the applied analytical methods enabled the identification of bsAb1 heterogeneous charge variants; however, the assignment of HC2-D106-iso to a specific CEX fraction was not possible, since all offline fractions exhibited similar quantities. During this comprehensive bsAb1 characterization, we observed that the isolated offline fractions still contained coelution variant peaks (Supporting Information Figure S1), even though precise sampling at the peak maxima was performed, which complicated the peak identification.

Online Characterization of bsAb1 Charge Variants. As a next step, we aimed to fully automate the characterization workflow of bsAb1 charge variants by developing a mD-LC-MS system consisting of online fractionation followed by analysis at the reduced (2D-LC-MS) and peptide level (4D-LC-MS). Figure 2 details the two different online mD-LC-MS setups. The 2D-LC-MS configuration incorporates [1]D CEX separation identical with the applied release testing method followed by online sampling of charge variant peaks, one-by-one [2]D RPLC based desalting, reduction, and subsequent RPLC (C4) separation followed by MS detection. The 4D-LC-MS setup incorporates the same [1]D CEX separation followed by online charge variant peak collection, [2]D RPLC (C3) based desalting and reduction, [3]D tryptic digestion, and [4]D RPLC-MS/MS peptide mapping.

At first, the bsAb1 charge variants were analyzed with the 2D-LC-MS setup. The online [1]D CEX UV chromatogram (Figure 3) is well comparable to the analytical release data (Figure 1) demonstrating a successful method transfer. In comparison with the offline fractions, we were able to collect the peak maxima much more precisely (online sampling times of 7−9 s). This is of importance because the coelution of offline fractionated bsAb1 and complex charge variant patterns impair correct peak assignment. In contrast, mD-LC-MS allows the consecutive characterization of coeluting product variants within one analysis. More detailed online captured cuts were stepwise transferred to a RP column for desalting, reduction, and separation of LCs and HCs followed by MS detection.

The 11 most abundant cuts were further analyzed, whereby cuts A1−A6 are from the acidic region, B1−B4 cover the basic region, and MP corresponds to the main peak region. It is important here to highlight that further cuts in between helped to monitor and evaluate the enrichment and depletion of coeluting peaks before and after the different peak maxima, exemplarily shown in Supporting Information Figure S3. An increase in the intensity of the corresponding charge variant species of cuts toward the peak maxima and a decrease of the sloping cuts can be observed. Hence, this underlines the high granularity of the methodology in terms of precise narrow cuts resulting in highly enriched molecular variants facilitating the identification and more detailed assignment of bsAb1 modifications in contrast to the obtained offline data.

The developed 2D-LC-MS approach identified all bsAb1 charge variants detected by the offline fraction combined with subsequent near-native SEC-UV-MS and reduced RP-MS analysis. Figure 3 illustrates the online 2D-LC-MS cuts and shows exemplarily [2]D total ion current chromatograms and deconvoluted mass spectra for the LC1-LC2 dimer (CEX Cut A1), the 2xLC1-bsAb1 (Cut A2), and the Fab glycosylation (Cut A3) species. Further identified variants are summarized in Supporting Information Figure S4. Supporting Information Table S4 summarizes the observed and theoretical masses of the identified bsAb1 variants (<3 Da mass difference). Worth mentioning is the identification of the low abundant (<0.2%)

https://doi.org/10.1021/jasms.2c00296
J. Am. Soc. Mass Spectrom. 2022, 33, 2319−2327

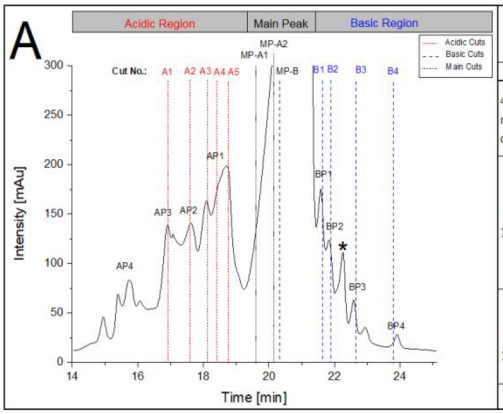

B

4D peptide-mapping column	Online 4D-LC-MS Cut No.	CEX Peak Name	N-/C-Terminal Variants (%) HC2-Q1	HC2-Q1-VHS	HC1'HC2-Cterm-PN	HC1'HC2-Cterm-K	Deamidation and Isomerization Variants (%) HC1'HC2-N390/395'N400/405-deam	HC2-D106-iso	LC2-D50-iso	LC2-D50-suc	Additional Variants (%) HC2-M124-ox	HC1'HC2-N321'N331-deam	HC1'HC2-M434'M444-ox
RPLC Poroshell 120 Bonus-RP	A1	AP3	e.e.	e.e.	e.e.	e.e.	3.0	5.2	n.s.	n.s.	1.1	0.8	0.8
	A2	AP2	e.e.	e.e.	e.e.	e.e.	2.7	5.4	n.s.	n.s.	1.8	0.7	0.7
	A3	AP1	e.e.	e.e.	e.e.	e.e.	3.3	6.7	n.s.	n.s.	2.1	0.7	0.7
	A4	AP1	e.e.	e.e.	e.e.	e.e.	6.5	5.4	n.s.	n.s.	2.1	0.7	0.6
	A5	AP1	e.e.	e.e.	e.e.	e.e.	5.2	4.2	n.s.	n.s.	1.6	0.8	0.5
	MP-A1	MP	e.e.	e.e.	e.e.	e.e.	0.9	5.6	n.s.	n.s.	2.4	0.4	0.9
	MP-A2	MP	e.e.	e.e.	e.e.	e.e.	1.3	5.5	n.s.	n.s.	0.9	0.6	1.4
	MP-B	MP	0.8	0.2	0.6	n.d.	n.s.	n.s.	0.1	1.8	1.2	0.4	0.3
RPLC Poroshell 120 SB-C18	B1	BP1	49.6	1.5	7.0	n.d.	n.s.	n.s.	0.6	1.9	2.5	0.5	2.2
	B2	BP2	5.9	2.4	19.6	n.d.	n.s.	n.s.	1.0	2.3	3.9	0.7	1.2
	B3	BP3	1.8	37.5	3.2	n.d.	n.s.	n.s.	7.2	6.8	3.2	0.9	1.4
	B4	BP4	0.4	n.d.	2.2	2.7	n.s.	n.s.	0.5	1.1	1.5	0.3	0.7

Figure 4. 4D-LC-MS analysis of bsAb1. (A) CEX-UV chromatogram of online 4D-LC-MS highlighting collected cuts (sampling time: 9 s): red lines: cuts of acidic charge variants (A1-A5); blue lines: cuts of basic charge variants (B1−B4); black lines: cuts of main peak (MP-A1, MP-A2 and MP-B), including analytical CEX peak naming (black). (B) Relative quantification (%) of bsAb1 PTMs. *This study was performed prior to the final manufacturing process; this peak is almost depleted upon application of the final purification process. ee = early elution within injection peak, nd = not detected, ns = not separated from wild type peptide.

AP5 species as the LC1-LC2 dimer (Cut A1) which could not be assigned by the conventional offline fractionation approach.

As can be depicted from Figure 3B, both bsAb1 LCs were separated on the C4 column whereas almost no HC signals (intensity <2e4) were detected, proving the presence of the LC1−LC2 dimer. The covalent disulfide bridge was verified by offline native LysC peptide mapping as described before. Furthermore, the precise online cuts enabled the assignment of 2xLC1-bsAb1 (Cut A2), indicated by an almost complete decrease in LC2 abundancy to the more acidic (left) side of AP4, and the disialylated (S2) Fab glycosylation (Cut A3) to the more basic (right) side of AP4 (Figure 3). Interestingly, the Fab glycosylation (G2S2F) was observed to elute separately within an additional LC2 peak shoulder (Figure 3B). Moreover, the left side AP3 peak also contained disialylated (S2) Fc glycans (Cut A4), correspondingly as observed for disialylated Fab glycosylation eluting separately (peak shoulder) on C4 column, whereas the right peak side of AP3 showed low levels of monosialylated (S1) Fab glycosylation (Cut A5) without separation (Supporting Information Figure S4). Likewise, the monosialylated (S1) Fc glycosylation of AP1 was confirmed by 2D-LC-MS (Cut A6). Finally, all basic charge species predominantly containing N- and C-terminal modifications were identified, with the exception of isobaric LC2-D50-iso variant and the low-level C-terminal lysine (~5% in offline peptide mapping), which is in agreement with the data from the offline fractionation approach.

In comparison to the reduced RP-MS of the manually isolated fractions, all charge variants were verified, and even one more was found (LC1−LC2 dimer). Moreover, the concise online sampling facilitated the more precise assignment of bsAb1 charge variants. However, to identify the remaining CEX peak variants LC-MS/MS peptide mapping is required to resolve the amino acid sequence as well as the location of modifications.[23] Nor could modifications with no or low mass difference (e.g., isomerization, deamidation) be identified at a reduced level. Hence, an additional assessment at the peptide level by 4D-LC-MS was subsequently conducted.

Figure 4A illustrates the online 4D-LC-MS CEX UV chromatogram of bsAb1, exhibiting slightly lower peak resolution compared to 2D-LC-MS and the release testing methods (Figures 1 and 3). This can be explained by the application of an increased protein load (1000 μg compared to 150 μg, Supporting Information Figure S5) ensuring good intensities for further dimensions. It should be mentioned that the 4D-LC-MS analysis was performed with drug substance material prior to the establishment of the final manufacturing process. Hence, the increased basic peak eluting at around 22.2 min (marked by an asterisk) is almost depleted upon application of the final purification process and was thus not further assessed for the final reference material (Figure 1).

Twelve peak cuts were transferred from ^{1}D to desalting and reduction on the RP column and subsequently digested using an online trypsin cartridge with optimized ACN concentration (Supporting Information Figure S6), separated on one of two different RP columns, and finally analyzed by MS/MS. Cuts A1−A5 are from the acidic region, cuts B1−B4 cover the basic region, and MP-A1, MP-A2, and MP-B correspond to the main peak region. Further optimization of peptide separation was required to enable assessment of the aspartate isomerization sites (LC2-D50-iso and HC2-D106-iso) that have been previously identified as CQAs[24] while ensuring a low back pressure for the trypsin cartridge. A previous study applying thermal and physiological stress conditions showed an increase of HC2-D106-iso for the acidic region peaks (predominantly AP1 and AP2), whereas LC2-D50-iso was found to be increased in BP3.[24] Hence, acidic peaks MP-A1 and MP-A2 were analyzed on an RPLC Poroshell 120 Bonus-RP separating HC2-D106-iso, whereas an additional 4D-LC-MS run for the basic cuts and MP-B was conducted implementing a RPLC Poroshell 120 SB-C18 column within ^{4}D to separate the modified peptide LC2-D50-iso from its wild type. Be aware that some further PTMs do not separate or elute early (Figure 4B) on one of the RP columns, but the combination of the two chosen columns enables the quantification of all important bsAb1 PTMs depending on their occurrence within either the acidic or basic region. The application of two different RP columns increases the capability for the detection of peptide modifications with no or low mass differences such as aspartate isomerization or asparagine deamidation. This is, to the best of our knowledge, the first time that different RP columns compared to the already reported setup[25] are introduced to ensure chromatographic separation of multiple PTMs. Another

https://doi.org/10.1021/jasms.2c00296
J. Am. Soc. Mass Spectrom. 2022, 33, 2319−2327

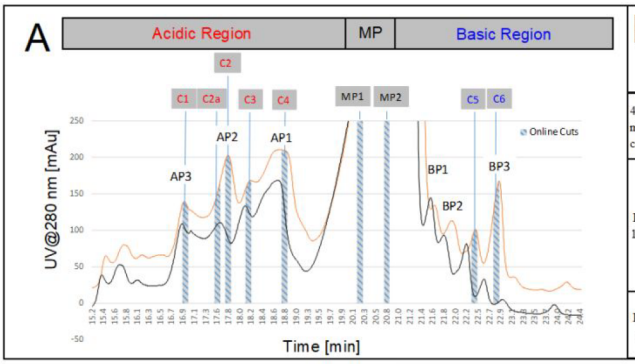

B

			DP Release			DP Stability		
			Isomerization and Succinimide Variants (%)			Isomerization and Succinimide Variants (%)		
4D peptide mapping column	Online 4D-LC-MS Cut No.	CEX Peak Name	HC2-D106-iso	LC2-D50-iso	LC2-D50-suc	HC2-D106-iso	LC2-D50-iso	LC2-D50-suc
RPLC Poroshell 120 Bonus-RP	C1	AP3	5.2	n.a.	n.a.	7.7	1.8	2.3
	C2a	AP2	n.d.	n.a.	n.a.	15.1	n.a.	n.a.
	C2	AP2	5.4	0.6	1.8	10.9	1.4	2.3
	C3	AP1	6.7	n.a.	n.a.	12.9	1.6	2.2
	C4	AP1	4.2	n.a.	n.a.	7.5	1.7	2.5
	MP1	MP	11	0.1	1.8	18.1	2.6	3.6
	MP2	MP	8.5	0.1	4.2	12.9	1.0	1.8
RPLC Poroshell 120 SB-C18	C5	BP2-3	2.2	2.1	3.0	4.7	7.9	6.1
	C6	BP3	1.5	11.2	6.8	3.7	49.0	35.8

Figure 5. Drug product stability study. (A) Overlay of CEX-UV chromatogram of bsAb1 drug product at initial release level (black line) and after storage for 30 months at 5 °C (orange line); online 4D-LC-MS cuts (sampling time: 9 s) within DP stability are highlighted in blue-gray, whereas acidic charge variants (C1−C4) are highlighted in red, basic charge variants (C5 and C6) in blue, and cuts of main peak (MP1 and MP2) in black, including analytical CEX peak naming. (B) Relative quantification (%) of bsAb1 PTMs of DP release (highlighted in black) and stability material (highlighted in orange)

report on workflow optimization for peptide mapping describes the improved retention of hydrophilic peptides.[26] More recently, the implementation of a precolumn reducing the back pressure and thus enabling the application of any offline analytical C18 method was reported and will improve further 4D-LC-MS investigations.[27]

To demonstrate the performance of the developed 4D-LC-MS workflow, the sequence coverages, number of identified amino acids, and TIC intensities for CEX main peaks MP-A1 and MP-B were analyzed in comparison to the recorded offline MP fraction (Supporting Information Table S5). Sequence coverage for acidic cuts (MP-A1) was lower (>90%) compared to the offline fractionation approach (>98%), whereas basic cuts (MP-B) showed comparable coverages (>95%). Generally, the fast turn-around time of the online tryptic digestion (less than 30 s compared to 18 h for offline digestion) resulting in a less effective digestion and lower TIC intensities as well as starting conditions at higher acetonitrile concentration resulting in the loss of shorter hydrophilic peptides explain these differences. A previous experiment[25] applying similar 4D-LC-MS conditions showed equivalent sequence coverages of approximately 96% in comparison to the online basic cuts (>95%) but lower for the analysis of acidic cuts (>90°) indicating an impact of the different implemented peptide mapping columns. Altogether, the developed 4D-LC-MS setup guarantees sufficient peptide intensities, showing relatively high sequence coverages (>90%) and more importantly separating all relevant PTMs for charge variant identification and quantification.

Subsequently, bsAb1 PTMs were quantified as summarized in Figure 4B. Acidic charge variants were identified in accordance with the described offline fractionation approach. For AP1 an enrichment of the deamidated Fc motif, HC1'HC2-N390/395'N400/405-deam was observed. However, as already observed for the offline peptide mapping experiments no specific peak assignment for HC2-D106-iso was feasible, since similar levels for all acidic cuts were detected. As described previously, this degradation site was identified as CQA[24] and hence led us to a further mD-LC-MS investigation of real-time stability material which we will describe in more detail later. Likewise, the bsAb1 basic variants were verified successfully by the automated online 4D-LC-MS setup: BP1 comprises around 50% glutamine (Cut B1), whereas BP2 contains C-terminal proline amidation (~20%, Cut B2), BP3 shows LC2-D50-iso and the respective succinimide intermediate (Cut B3, ~7% for both sites), whereas BP4 contains the C-terminal lysine (~3%, Cut B4). Only the observed enrichment in C-terminal proline amidation for BP4 previously confirmed by 2D-LC-MS (at both HCs) and the offline peptide-mapping approach (at ~70%) could not be verified.

Apart from this, the quantified PTMs in-between the herein developed automated online bottom-up approach (Figure 4B) applying narrow cuts assigned the same bsAb1 charge species to CEX peaks in agreement with the broader offline fractions (Supporting Information Table S3). Differences of quantification between both approaches can be explained by the divergent fraction window of CEX peaks. Hence, broader windows for the offline fractionation as a consequence contain more coeluting species but show consistently high intensity mass spectra as these were concentrated and the same amount of protein was applied for peptide mapping. In contrast, the online approach facilitates more precise cuts enriched with selected charge variants but generally comprises lower and varying concentrations due to the lower amounts of applied protein and further depends on the CEX peak intensity as well as contiguous dimensions. This may result in less intensive mass spectra as well as differences in ionization efficacies depending on the protein/peptide concentration. In contrast, longer sample handling times during the offline approach might include method artifacts.

In order to investigate method-induced artifacts in comparison to the offline approach, an asparagine spot known to be prone to deamidation during the procedure of peptide mapping (HC1'HC2-N321'N331-deam)[22] and two susceptible methionine oxidation spots (HC2-M124-ox, HC1'HC2-M434'M444-ox)[24] were assessed additionally (Figure 4B: Additional Variants). Particularly for the most susceptible oxidation site located in CDR (HC2-M124-ox) the online approach showed quantities around 1−4%, whereas the offline approach exhibited values roughly twice as high (3.4−7.8%, Supporting Information Table S2). This increase of oxidation for the classic approach can be explained by the different time-intensive manual fractionation, rebuffering and concentration steps. The other oxidation site (HC1'HC2-M434'M444-ox), a known conserved Fc motif, demonstrated comparable low quantities for both workflows. HC1'HC2-N321'N331-deam (Fc motif) exhibits similarly low levels for

https://doi.org/10.1021/jasms.2c00296
J. Am. Soc. Mass Spectrom. 2022, 33, 2319−2327

both approaches, indicating that offline and on-column tryptic digests both show low levels of artificial peptide modifications. This is in agreement to an earlier publication, which deduced less method-induced variants for online 4D-LC-MS.[25]

Next, we aimed for an identification and assignment of the degradation variant HC2-D106-iso in the acidic peak cut area. The relative low level of HC2-D106-iso in bsAb1 reference material, the complex CEX profile, and moderate isomerization levels detected for all fractions/cuts did not allow the direct assignment to a specific CEX peak (Figure 4 and Supporting Information Table S2). However, a drug product stability sample stored at 5 °C for 30 months showed an increase of isomerization at HC2-D106 and the CEX UV acidic peak 2 (AP2), compared to the starting material (0 months, Supporting Information Table S6).

As described before, LC2-D50-iso and the corresponding LC2-D50-suc have already been confirmed to elute in BP3 (within the offline and online approach, respectively). Precise 4D-LC-MS cuts of a drug product (DP) release and stability sample were subsequently examined (Figure 5, showing exemplarily the precise online sampling cuts). Indeed, the analysis verified the correct identification of BP3 containing LC2-D50-iso and LC2-D50-suc (DP stability cut C6:49.0% LC2-D50-iso and 35.8% LC2-D50-suc). For all investigated acidic and main peak cuts of DP release and stability material, similar and increased levels of HC2-D106-iso content were observed for the long-term stored bsAb1 stability sample. However, only the left peak shoulder of AP2 (Cut C2a: 15.1%) and main peak (Cut MP1:18.1%) of the DP stability sample exhibited a more pronounced enrichment of HC2-D106-iso, indicating a correlation between HC2-D106-iso formation and elevated AP2 levels following the storage conditions (Figure 5A). Consequently, the data suggests that AP2 can be utilized to monitor HC2-D106-iso formation at release testing level using CEX-UV detection.

These data demonstrate another great benefit of mD-LC-MS: fast, automated, and easy follow-up analysis of additional samples exhibiting new or increasing peak variants. Together with the advantage of the application of lower amounts of proteins, generating less method induced artifacts, the possibility to collect the peak maxima more precisely, the availability to switch fast in-between different set-ups and/or protein-levels, as well as faster turn-around times makes the online mD-LC-MS setup a favored method. Overall, the mD-LC-MS/MS method facilitates the detailed characterization of a broad range of product variants within days compared to offline fraction/characterization approaches, which require several weeks for sampling followed by stepwise analysis.

CONCLUSIONS

In-depth characterization of therapeutic antibody variants is required for monitoring relevant product attributes ensuring their efficacy and safety, particularly with regard to the increasing complexity of their variant profiles. Hence, for the first time we developed a mD-LC-MS setup for the characterization of a bispecific antibody format exhibiting a complex, highly heterogeneous charge variant profile to challenge its performance in a direct comparison with an offline fractionation and analytical characterization workflow.

The evolved online mD-LC-MS at reduced (2D-) and peptide-level (4D-LC-MS) allows us to identify and monitor multiple charge variants at the space-resolved/amino acid level. Compared to the offline fractionation and analytical characterization approach, our results demonstrate a reduced total analysis and laboratory working time, reduction of required protein amount, less method induced artifacts, and identification of low abundant product variants. However, offline fractionation of protein variants is currently still required to allow the separate functional and safety testing of product-related attributes. On the other hand, the development and application of column combination (e.g., CEX-RPLC separation with UV and/or MS detection) or new functional testing columns (e.g., for testing Fc effector functions) could be implemented in the mD-LC-MS setup to overcome this actual limitation. Nevertheless, the mD-LC-MS approach features the opportunity to overcome current limitations of the multi attribute monitoring testing by LC-MS peptide mapping (MAM) at a reduced peptide level. The main challenge of introducing MAM in the control strategy of biologics is mainly related to linking analytical data from conventional release testing methods at intact levels to reduced peptide mapping results of MAM. In conclusion, mD-LC-MS allows simultaneous attribute monitoring at the intact protein and reduced peptide level and therefore adds value to the development and validation of MAM testing approaches.

ASSOCIATED CONTENT

Supporting Information

The Supporting Information is available free of charge at https://pubs.acs.org/doi/10.1021/jasms.2c00296.

Additional experimental details, methods and data (PDF)

AUTHOR INFORMATION

Corresponding Author

Ingrid Grunert − *Pharma Technical Development, Roche Diagnostics GmbH, 82377 Penzberg, Germany;* orcid.org/0000-0002-5596-1015; Phone: +4988566012918; Email: ingrid.grunert@roche.com

Authors

Katrin Heinrich − *Pharma Technical Development, Roche Diagnostics GmbH, 82377 Penzberg, Germany*

Michael Hingar − *Pharma Technical Development, Roche Diagnostics GmbH, 82377 Penzberg, Germany*

Juliane Ernst − *Pharma Technical Development, Roche Diagnostics GmbH, 82377 Penzberg, Germany*

Martin Winter − *Pharma Technical Development, Roche Diagnostics GmbH, 82377 Penzberg, Germany*

Katrin Bomans − *Pharma Technical Development, Roche Diagnostics GmbH, 82377 Penzberg, Germany*

Katharina Wagner − *Pharma Technical Development, Roche Diagnostics GmbH, 82377 Penzberg, Germany*

Arnaud Fevre − *Pharma Technical Development, Hoffmann-La Roche, 4070 Basel, Switzerland;* orcid.org/0000-0001-6536-9384

Dietmar Reusch − *Pharma Technical Development, Roche Diagnostics GmbH, 82377 Penzberg, Germany*

Manfred Wuhrer − *Center for Proteomics and Metabolomics, Leiden University Medical Center, 2333 Leiden, The Netherlands;* orcid.org/0000-0002-0814-4995

Patrick Bulau − *Pharma Technical Development, Hoffmann-La Roche, 4070 Basel, Switzerland;* orcid.org/0000-0002-7121-2954

Complete contact information is available at:
https://pubs.acs.org/10.1021/jasms.2c00296

Author Contributions

I.G., K.H., M.H., J.E., M.Wi., K.W., and A.F. performed experiments and data analysis. I.G. wrote the manuscript. M.Wu., D.R. and P.B. reviewed the manuscript.

Notes

The authors declare no competing financial interest.

■ ACKNOWLEDGMENTS

We are indebted to all members of the laboratories at Roche in Penzberg for valuable discussions.

■ REFERENCES

(1) Kintzing, J. R.; Filsinger Interrante, M. V.; Cochran, J. R. Emerging Strategies for Developing Next-Generation Protein Therapeutics for Cancer Treatment. *Trends Pharmacol. Sci.* **2016**, *37* (12), 993−1008.
(2) Carter, P. Bispecific human IgG by design. *J. Immunol. Methods* **2001**, *248* (1−2), 7−15.
(3) Schaefer, W.; Regula, J. T.; Bahner, M.; Schanzer, J.; Croasdale, R.; Durr, H.; Gassner, C.; Georges, G.; Kettenberger, H.; Imhof-Jung, S.; Schwaiger, M.; Stubenrauch, K. G.; Sustmann, C.; Thomas, M.; Scheuer, W.; Klein, C. Immunoglobulin domain crossover as a generic approach for the production of bispecific IgG antibodies. *Proc. Natl. Acad. Sci. U. S. A.* **2011**, *108* (27), 11187−92.
(4) Ridgway, J. B.; Presta, L. G.; Carter, P. 'Knobs-into-holes' engineering of antibody CH3 domains for heavy chain heterodimerization. *Protein Eng.* **1996**, *9* (7), 617−21.
(5) Haberger, M.; Leiss, M.; Heidenreich, A. K.; Pester, O.; Hafenmair, G.; Hook, M.; Bonnington, L.; Wegele, H.; Haindl, M.; Reusch, D.; Bulau, P. Rapid characterization of biotherapeutic proteins by size-exclusion chromatography coupled to native mass spectrometry. *mAbs* **2016**, *8* (2), 331−9.
(6) Beck, A.; Wagner-Rousset, E.; Ayoub, D.; Van Dorsselaer, A.; Sanglier-Cianferani, S. Characterization of therapeutic antibodies and related products. *Anal. Chem.* **2013**, *85* (2), 715−36.
(7) Du, Y.; Walsh, A.; Ehrick, R.; Xu, W.; May, K.; Liu, H. Chromatographic analysis of the acidic and basic species of recombinant monoclonal antibodies. *mAbs* **2012**, *4* (5), 578−85.
(8) Chen, Z.; Zeng, M.; Park, S. J.; Balakrishnan, G.; Zhou, K.; Pan, D.; Das, T. K. Bridging size and charge variants of a therapeutic monoclonal antibody by two-dimensional liquid chromatography. *J. Pharm. Biomed. Anal.* **2020**, *183*, 113178.
(9) Camperi, J.; Goyon, A.; Guillarme, D.; Zhang, K.; Stella, C. Multi-dimensional LC-MS: the next generation characterization of antibody-based therapeutics by unified online bottom-up, middle-up and intact approaches. *Analyst* **2021**, *146* (3), 747−769.
(10) Graf, T.; Heinrich, K.; Grunert, I.; Wegele, H.; Haberger, M.; Bulau, P.; Leiss, M. Recent advances in LC-MS based characterization of protein-based bio-therapeutics - mastering analytical challenges posed by the increasing format complexity. *J. Pharm. Biomed. Anal.* **2020**, *186*, 113251.
(11) Iguiniz, M.; Heinisch, S. Two-dimensional liquid chromatography in pharmaceutical analysis. Instrumental aspects, trends and applications. *J. Pharm. Biomed. Anal.* **2017**, *145*, 482−503.
(12) Pirok, B. W. J.; Stoll, D. R.; Schoenmakers, P. J. Recent Developments in Two-Dimensional Liquid Chromatography: Fundamental Improvements for Practical Applications. *Anal. Chem.* **2019**, *91* (1), 240−263.
(13) Gstottner, C.; Klemm, D.; Haberger, M.; Bathke, A.; Wegele, H.; Bell, C.; Kopf, R. Fast and Automated Characterization of Antibody Variants with 4D HPLC/MS. *Anal. Chem.* **2018**, *90* (3), 2119−2125.
(14) Goyon, A.; Dai, L.; Chen, T.; Wei, B.; Yang, F.; Andersen, N.; Kopf, R.; Leiss, M.; Molhoj, M.; Guillarme, D.; Stella, C. From proof of concept to the routine use of an automated and robust multi-dimensional liquid chromatography mass spectrometry workflow applied for the charge variant characterization of therapeutic antibodies. *J. Chromatogr. A* **2020**, *1615*, 460740.
(15) Haberger, M.; Heidenreich, A. K.; Hook, M.; Fichtl, J.; Lang, R.; Cymer, F.; Adibzadeh, M.; Kuhne, F.; Wegele, H.; Reusch, D.; Bonnington, L.; Bulau, P. Multiattribute Monitoring of Antibody Charge Variants by Cation-Exchange Chromatography Coupled to Native Mass Spectrometry. *J. Am. Soc. Mass Spectrom.* **2021**, *32* (8), 2062−2071.
(16) Dutta, D.; Mandal, C.; Mandal, C. Unusual glycosylation of proteins: Beyond the universal sequon and other amino acids. *Biochim. Biophys. Acta, Gen. Subj.* **2017**, *1861* (12), 3096−3108.
(17) Phung, W.; Han, G. H.; Polderdijk, S. G. I.; Dillon, M.; Shatz, W.; Liu, P.; Wei, B. C.; Suresh, P.; Fischer, D.; Spiess, C.; Bailey, A.; Carter, P. J.; Lill, J. R.; Sandoval, W. Characterization of bispecific and mispaired IgGs by native charge-variant mass spectrometry. *Int. J. Mass Spectrom.* **2019**, *446*, 116229.
(18) Li, H.; Er Saw, P.; Song, E. Challenges and strategies for next-generation bispecific antibody-based antitumor therapeutics. *Cell. Mol. Immunol.* **2020**, *17* (5), 451−461.
(19) Reusch, D.; Haberger, M.; Falck, D.; Peter, B.; Maier, B.; Gassner, J.; Hook, M.; Wagner, K.; Bonnington, L.; Bulau, P.; Wuhrer, M. Comparison of methods for the analysis of therapeutic immunoglobulin G Fc-glycosylation profiles-Part 2: Mass spectrometric methods. *mAbs* **2015**, *7* (4), 732−742.
(20) Sinha, S.; Pipes, G.; Topp, E. M.; Bondarenko, P. V.; Treuheit, M. J.; Gadgil, H. S. Comparison of LC and LC/MS methods for quantifying N-glycosylation in recombinant IgGs. *J. Am. Soc. Mass Spectrom.* **2008**, *19* (11), 1643−54.
(21) Schmid, I.; Bonnington, L.; Gerl, M.; Bomans, K.; Thaller, A. L.; Wagner, K.; Schlothauer, T.; Falkenstein, R.; Zimmermann, B.; Kopitz, J.; Hasmann, M.; Bauss, F.; Haberger, M.; Reusch, D.; Bulau, P. Assessment of susceptible chemical modification sites of trastuzumab and endogenous human immunoglobulins at physiological conditions. *Commun. Biol.* **2018**, *1*, 28.
(22) Diepold, K.; Bomans, K.; Wiedmann, M.; Zimmermann, B.; Petzold, A.; Schlothauer, T.; Mueller, R.; Moritz, B.; Stracke, J. O.; Molhoj, M.; Reusch, D.; Bulau, P. Simultaneous assessment of Asp isomerization and Asn deamidation in recombinant antibodies by LC-MS following incubation at elevated temperatures. *PLoS One* **2012**, *7* (1), No. e30295.
(23) Sandra, K.; Vandenheede, I.; Sandra, P. Modern chromatographic and mass spectrometric techniques for protein biopharmaceutical characterization. *J. Chromatogr. A* **2014**, *1335*, 81−103.
(24) Grunert, I.; Heinrich, K.; Ernst, J.; Hingar, M.; Briguet, A.; Leiss, M.; Wuhrer, M.; Reusch, D.; Bulau, P. Detailed Analytical Characterization of a Bispecific IgG1 CrossMab Antibody of the Knob-into-Hole Format Applying Various Stress Conditions Revealed Pronounced Stability. *ACS Omega* **2022**, *7*, 3671.
(25) Camperi, J.; Grunert, I.; Heinrich, K.; Winter, M.; Ozipek, S.; Hoelterhoff, S.; Weindl, T.; Mayr, K.; Bulau, P.; Meier, M.; Molhoj, M.; Leiss, M.; Guillarme, D.; Bathke, A.; Stella, C. Inter-laboratory study to evaluate the performance of automated online characterization of antibody charge variants by multi-dimensional LC-MS/MS. *Talanta* **2021**, *234*, 122628.
(26) Pot, S.; Gstottner, C.; Heinrich, K.; Hoelterhoff, S.; Grunert, I.; Leiss, M.; Bathke, A.; Dominguez-Vega, E. Fast analysis of antibody-derived therapeutics by automated multidimensional liquid chromatography - Mass spectrometry. *Anal. Chim. Acta* **2021**, *1184*, 339015.
(27) Oezipek, S.; Hoelterhoff, S.; Breuer, S.; Bell, C.; Bathke, A. mD-UPLC-MS/MS: Next Generation of mAb Characterization by Multidimensional Ultra-Performance Liquid Chromatography Mass Spectrometry and Parallel On-column LysC & Trypsin Digestion. *Anal. Chem.* **2022**, *94* (23), 8136−8145.